Frontiers in Heat Pipes (FHP), 6, 2 (2015)
DOI: 10.5098/fhp.6.2

Global Digital Central
ISSN: 2155-658X

Frontiers in Heat Pipes

Available at www.ThermalFluidsCentral.org

AN EXPERIMENTAL PROCEDURE TO COMPARE THERMAL PERFORMANCE OF THERMOSYPHONS RAPIDLY

K. S. Ong* and Christopher Lim

Universiti Tunku Abdul Rahman, 31900 Kampar, Perak, Malaysia

ABSTRACT

There are various methods employed to determine the performance of heat pipes and two-phase closed thermosyphons. Perhaps the most common method involves measuring the rate of heat transfer from the evaporator to the condenser section with a water cooled jacket surrounding the latter. This entails higher costs and requires extended testing times. A method is proposed here to obtain comparative performance test data on various heat pipes rapidly and economically. The method does not require fabricating a water jacket. It merely involves measuring and comparing the transient temperature of a pre-heated container of hot water obtained first without the heat pipe and then with the heat pipe immersed into the container. The more efficient system will result in faster cooling of the container. The method is demonstrated using a number of different thermosyphons employing both water jackets and air cooled finned condensers. Their performances are compared in the paper.

Keywords: *Thermosyphon, comparative performance, rapid experimental procedure, air cooled condenser, water cooled condenser.*

1. INTRODUCTION

Heat pipes (HPs) are devices capable of transferring large quantities of heat effectively and efficiently. A HP typically consists of a sealed container lined with a wicking material. The container is evacuated and filled with just enough liquid to fully saturate the wick. A wickless HP is also known as a thermosyphon, shown in Fig.1. Heat applied to the evaporator section causes it to boil and vaporize, picking up latent heat of vaporization. The vapor then rises to the condenser section where it condenses. Here vapor gives up its latent heat of condensation. The condensate then travels back to the evaporator section of the heat pipe by gravity or capillary action. The performance of HPs depend on various factors such as type of fill liquid, fill ratio (FR), heat input at the evaporator section, inclination and physical dimensions of the pipe.

The performance of a HP could be evaluated by determining the amount of heat input at the evaporator section or by measuring the heat transferred at the condenser section to the coolant. At steady state, these two heat transfer rates should be equal if there is no heat loss from the pipe. In order to compare the performances of various heat pipes the heat transfer rates could be plotted against the temperature difference between the evaporator and condenser sections. This would give an indication of the thermal resistance of the pipe. A high thermal resistance would indicate a poor performing HP and vice versa.

Ong et al. (2014) investigated the performance of water and R410a filled thermosyphon at various power inputs (100 to 830 W), fill ratios (0.25 to 0.93) and inclinations (30º to 90º). The authors used a 38 mm OD x 807 mm long thermosyphon with a 71 mm OD cooling water jacket and electrical heating bands to supply heat to the evaporator section. By plotting input power against temperature difference between evaporator and condenser sections, found that the R410a filled thermosyphon performed better in the vertical position at all FR's and that the water filled thermosyphon performed better at low FR and when inclined. They showed that the evaporator wall temperature was not uniform especially at high power inputs, low fill ratios and large inclinations.

Shanthi and Velraj (2014) experimented with a two phase gravity assisted thermosyphon. The authors used a 12.5 mm ID x 300 mm long thermosyphon with a 200 mm long cooling water jacket and a 1000 W nichrome heating wire wound around the 75 mm long evaporator section. They measured the performance of their thermosyphon by plotting efficiency defined as ratio of power output over power input, versus power input and obtained values as high as 0.9. Anjakar and Yarasu (2012) determined the effect of condenser length on the performance of thermosyphon by using a 32 mm OD x 1000 mm long thermosyphon with a 450 mm long water cooled jacket and a 300 mm long nichrome heating element at the evaporator section. The authors determined the efficiency using the ratio of heat conducted away by the coolant water at the condenser section to the power input at the evaporator section and found values of 0.5 to 0.95. In theory the ratio should be equal to 1.0.

Buschmann and Franzke (2013) compared the performance of thermosyphons filled with deionised water (DI) and titanium oxide-based DI water and gold nanofluid. They showed that the nanofluids reduced thermal resistances up to 24 %. They also noted that nanoparticles depositing on the evaporator wall after prolonged heating operations resulted in an absence of nanoparticles being transported to the condenser section that eventually reduced the thermal transport capacity of the nanofluid and increased the overall thermal resistance. Huminic et al. (2011) experimented with thermosyphons filled with iron oxide nano particles and found that a concentration level of 5.3 % improved the thermal performance of their HP. Solomon et al. (2012) determined the thermal performance of a heat pipe with a nano particles-coated wick. They found that the thermal resistance reduced from 0.32 to 0.11 ºC/W when subjected to power input ranging from 100 to 200 W, respectively.

Qu and Wang (2013) showed that the thermosyphon with a FR of 40 to 50 % resulted in faster response time and lowest overall thermal resistance. Shabgard et al. (2014) studied the thermal characteristics of

* *Corresponding author. Email: skong@utar.edu.my*

Global Digital Central
ISSN: 2155-658X

HPs with different FRs. They showed that when the HP is underfilled, dry out occurs and that overfilling causes the overall thermal resistance to increase. The authors suggested that HPs should be filled slightly more than the optimal FR to prevent the breakdown of liquid film.

Qu and Wang (2013) showed that high heat flux results in lower thermal resistance of the evaporator section. Wang (2009) investigated the transient thermal performance of a bent HP with internal grooved surface and showed that straight pipes responded faster to high heat flux compared to bent shape HPs. Wang also found heat pipes have response times varies from 50 to180 s depending on the pipe angle from 0 to 140°.

HPs behave differently when inclined at different angles. Wang (2009) noted that with the increase in inclination, the temperature difference between the evaporator and condenser section increased. Huminic and Huminic (2011) investigated the heat transfer characteristics of two-phase closed thermosyphons using nanofluids. The authors plotted thermal resistance versus inclination angle to determine the performance of their HP. They found that water has the highest thermal resistance of 0.05 K/W compared to iron oxide nano-particles.

In their investigation on using heat pipes to enhance heat transfer during the charging and discharging rates of hydrogen in metal hydride tanks, Chung et al. (2013) found that the thermal resistance of their heat pipe ranged from 1.6 to 0.6 K/W at power inputs from 20 to 80 W.

Celata et al. (2010) investigated water filled stainless steel flat evaporators for space application. The authors plotted thermal resistance versus power input and found the overall thermal resistance decreased from 50.7 to 3.3 °C/W when power input increased from 20 to 80 W. Chang et al. (2012) investigated the thermal performance of two-phase water filled closed loop thermosyphons and plotted the thermal resistance versus power input. They found that the thermal resistance decreased from 0.30 to 0.05 K/W as the power input increased from 90 to 210 W. Solomon et al. (2013) determined the thermal performance of anodized two-phase closed thermosyphon by using a 16.5 mm ID x 350 mm long thermosyphon with a 150 mm long water cooled jacket and a 100 mm long resistance heater (1000W) at the evaporator section. The authors plotted the thermal resistance versus power input and found that the resistance reduced from 0.4 to 0.2 °C/W as power input increased from 50 to 250 W.

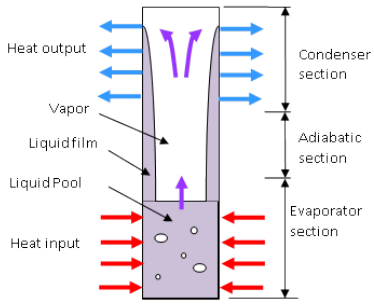

Fig. 1. Cross sectional view of a thermosyphon.

2. OBJECTIVE OF INVESTIGATION

All the experiments performed to determine the thermal performance of a thermosyphon involved measuring the rate of heat transfer from the evaporator to the condenser section via a water cooled jacket surrounding the latter. This entails high costs and requires extended testing times. A cheaper and quicker test method is required. This paper proposes a simple and quick method to obtain and to compare the performance of different types of thermosyphons.

3. METHODOLOGY

The proposed method involves, firstly, determining the transient temperature of an insulated container containing pre-heated hot water. Next the thermosyphon under investigation is inserted into the container and the temperature recorded. Heat is removed from the container by the thermosyphon throughout the cooling process and also through natural convection heat loss from the side walls of the container. The total heat removed from the container, $\dot{q}_b$, can be calculated from the transient bath temperature versus time results, viz.,

$$\dot{q}_b = W_b c_{pw} \left| \frac{dT_b}{d\theta} \right| \tag{1}$$

where, W_b is the weight of the water in the container, c_{pw} is the specific heat of water and $dT_b/d\theta$ is the rate of change of bath temperature with time.

In the case of a thermosyphon provided with a concentric pipe water cooling jacket, heat transfer from the condenser section, $\dot{q}_w$, of the thermosyphon to the cooling water is calculated from

$$\dot{q}_w = \dot{m}_w c_{pw} (T_{wo} - T_{wi}) \tag{2}$$

where, $\dot{m}_w$ is the mass flow rate of water, T_{wo} is the cooling water outlet temperature and T_{wi} is the inlet temperature.

The natural convection heat loss, $\dot{q}_{ins}$, from the container to the ambient can be estimated from

$$\dot{q}_{ins} = h_a A_{ins} (T_{ins} - T_a) \tag{3}$$

where, h_a is the natural convection heat transfer coefficient to the ambient, A_{ins} is the area of the insulation, T_{ins} is the insulation surface temperature and T_a is the surface ambient temperature.

The total heat removed from the container is the sum of the heat transfer to the coolant plus the natural convection heat loss, viz.,

$$\dot{q}_b = \dot{q}_w + \dot{q}_{ins} \tag{4}$$

A cooling index, γ, is introduced here, defined as the ratio of heat transfer to the coolant/total heat removed from the container, viz.,

$$\gamma = \frac{\dot{q}_w}{\dot{q}_b} \tag{5}$$

or

$$\gamma = \frac{\dot{q}_w}{\dot{q}_w + \dot{q}_{ins}} \tag{6}$$

In the absence of heat loss to the ambient, $\gamma = 1.00$.

The mean operating temperature difference between bath and coolant water is defined as

$$\Delta T_w = (T_b - T_w) \tag{7}$$

where, T_b is the mean bath temperature and T_w is the mean coolant water temperature defined by.

$$T_w = \frac{T_{wo} + T_{wi}}{2} \tag{8}$$

Global Digital Central
ISSN: 2155-658X

4. EXPERIMENTAL INVESTIGATION

The experimental set up is shown in Fig. 2. The equipment consisted of a 3.2 litre capacity hot water container (± 0.001 litre). All temperatures were measured using type T copper-constantan thermocouples (± 0.5 ^{o}C) connected to a data logger and logged every minute. Water temperature in the container was measured using two thermocouples immersed in the upper (280 mm from the base) and lower portions (90mm from the base) of the container. Temperature differences less than 3 ^{o}C were obtained. Mean container water temperature was taken as the arithmetic mean of the two positions. Two more thermocouples were attached to the outside of the insulated container to determine the external surface temperature of the container in order to calculate the natural convection heat loss from the external surface of the free-standing container. These thermocouples were insulated from the atmosphere by duct tape. Ambient temperature was measured with another thermocouple located nearby. Cross-pieces were attached to the top of each thermosyphon. It held a pressure gauge to measure the saturation pressure, a thermocouple to measure the saturation temperature and a filling valve. Inlet and outlet water temperatures were measured with thermocouples inserted inside the connecting plastic hoses of the cooling jacket. Experiments were conducted at two water flow rates, viz., at 0.9 and 50.0 ml/s (± 1 ml/s).

In order to demonstrate the effectiveness of the method, five copper thermosyphons were fabricated. Dimensions of the thermosyphon are shown in Table 1 and in Fig. 3 to Fig. 6. The first unit (HP # 1) is a water cooled type. The condenser section consisted of a 38 mm diameter x 127 mm long copper water cooled jacket. Thermocouples were mechanically attached to the adiabatic and condenser sections of the thermosyphons shown in Fig. 3 The second unit (HP # 2) is an air cooled type with a stainless steel spiral fin measuring 30 mm diameter x 0.5 mm thick stainless steel fins spaced 5 mm apart. The air cooled HPs # 3, 4, 5 were provided with parallel aluminum fins each 0.5 mm thick x 22.5 mm square x 2 mm pitch at the condenser section respectively. . The location of the thermocouples are shown in Figs. 4 to Fig. 6. Force air circulation rate was provided with an electric fan. Air flow was measured with a hot wire anemometer (± 0.1 m/s). For natural convection the fan was switched off.

Altogether eight experimental runs were conducted. The experimental procedure involved heating up the insulated container of water to a temperature of 100 ^{o}C and then allowing it to cool down. The water temperature was measured throughout the cooling process. Experiments were repeated by inserting and immersing the various thermosyphons to be tested into the container and measuring the temperature of the hot water as it cooled to 50 ^{o}C. Tests were conducted with various water flow rates and under natural or force air circulation. Each experimental run was repeated three times and the average results were obtained and plotted. Details of the test conditions under which the experiments were carried out are tabulated in Table 1.

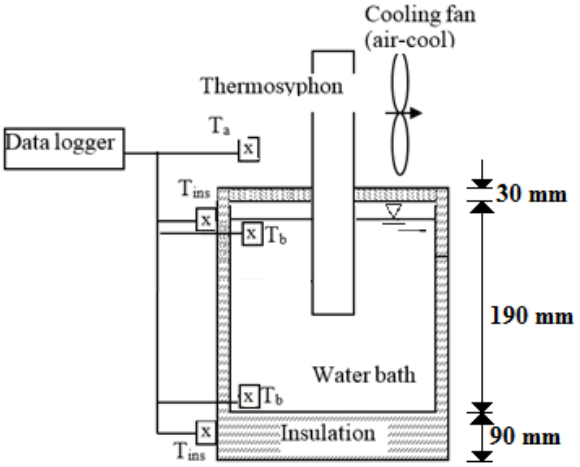

Fig. 2. Schematic of experimental set up.

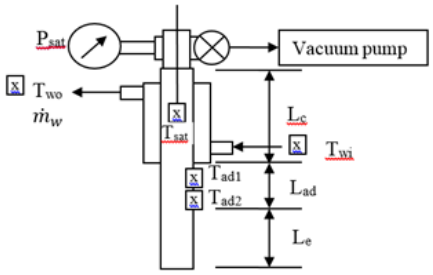

Fig. 3. Details of water cooled thermosyphon (HP1).

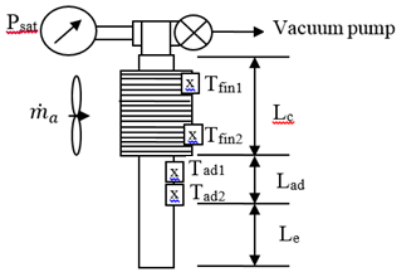

Fig. 4. Details of air cooled thermosyphon (HP2&3).

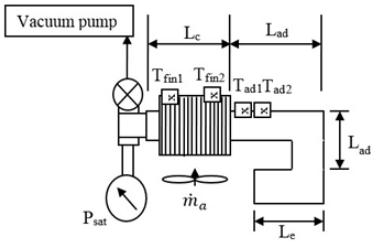

Fig. 5. Details of air cooled thermosyphon (HP4).

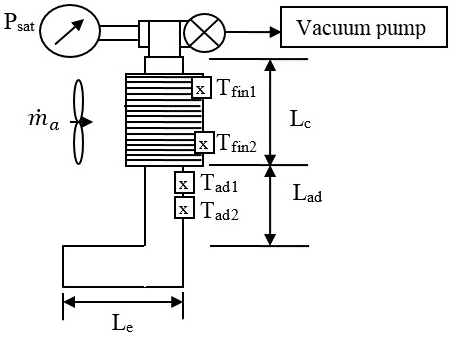

Fig. 6. Details of air cooled thermosyphon (HP5).

Table 1. Dimensions and experimental Runs conducted.

Run	HP #	Pipe shape	Coolant	Flow rate (ml/s)	D_e (cm)	L_e (cm)	L_c (cm)	L_{ad} (cm)	A_e (cm^2)	L_e / D_e	L_c / D_e	L_e / L_c
1	-	-	-	-	-	-	-	-	-	-	-	-
2	1	straight	water	0.9	2.54	12.7	12.7	5.0	101	5	5	1
3	1	straight	water	50.0	2.54	12.7	12.7	5.0	101	5	5	1
4	2	straight	air	0.0	1.2	12.7	12.7	5.0	48	11	11	1
5	2	straight	air	2.0	1.2	12.7	12.7	5.0	48	11	11	1
6	3	straight	air	2.0	0.9	12.7	25.4	5.0	36	14	28	0.5
7	4	J shape	air	2.0	0.9	12.7	25.4	75	36	14	28	0.5
8	5	L shape	air	2.0	0.9	12.7	25.4	75	36	14	28	0.5

5. EXPERIMENTAL RESULTS

5.1 Transient temperature

A typical set of transient temperature results obtained for Run 2 with minimum coolant flow rate of 0.9 ml/s is shown in Fig 7. Mean water container (T_b), coolant water inlet (T_{wi}), coolant water outlet (T_{wo}),

Global Digital Central
ISSN: 2155-658X

mean insulation (T_{ins}) and ambient temperatures are plotted. The results show that it took more than 3 hours for the water to be cooled down from 100°C to 50°C with the type HP1 thermosyphon. The experiment was stopped after 3.33 hours. A quadratic temperature-time relationship ($T_b = 0.0013\ \theta^2 - 0.47\ \theta + 95$) was obtained for the mean container temperature with a regression coefficient of 0.9866. The coolant water outlet temperature dropped from 72°C initially to 30°C after 3.33 hours. The temperature difference between inlet and outlet of the coolant water was about 44°C initially and about 5°C after 2 hours of cooling indicating that not much cooling could be performed when the container temperature dropped to below about 50°C.

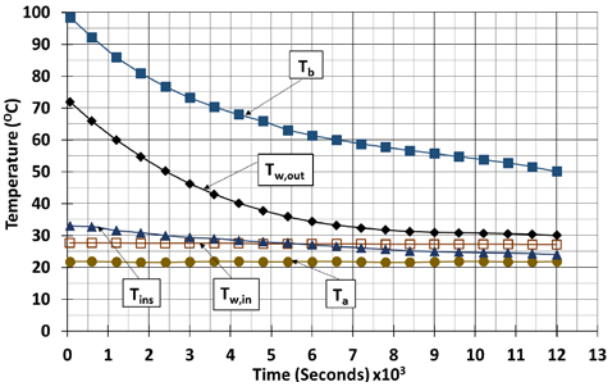

Fig. 7 Typical transient temperatures for Run 2

5.2 Heat transfer cooling rates

Typical heat transfer cooling rates for Run 2 are plotted in Fig. 8 for up to 2 hours of operation. The heat removed from the container ($\dot{q}_b$), heat transfer rate to the coolant water ($\dot{q}_w$) and the natural convection heat loss ($\dot{q}_{ins}$) are plotted together with the cooling index (γ). The results show that the cooling rate of the thermosyphon decreased with time or as the container cools which is to be expected. The heat loss from the container ($\dot{q}_{ins}$) is small. $\dot{q}_{ins}$ = 3 W at the start of the experiment with h_a = 1.5 W/m^{2}K. Towards the end of the experiment $\dot{q}_{ins}$ = 2 W with h_a = 1.5 W/m^{2}K. γ varied from 1.00 to 0.98. With h_a = 2.0 W/m^{2}K γ varied from 0.98 to 0.93. The variation in the γ factor is attributed to the value of h_a assumed to calculate for heat loss to the ambient.

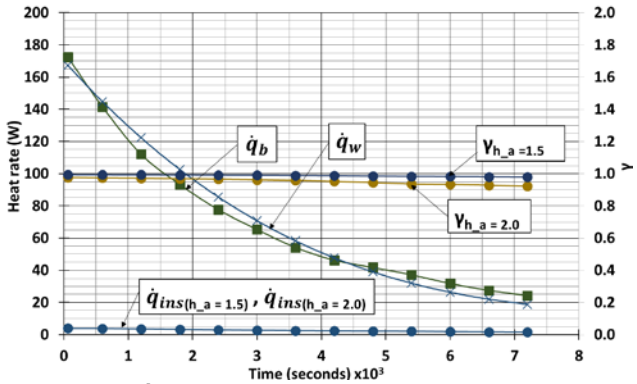

Fig. 8 Typical cooling heat rates for Run 2

5.3 Comparative performance of thermosyphons

The performances of the thermosyphons could be compared from the transient container temperature results shown plotted in Fig. 9. The rate at which container temperature decreases is a measure of the cooling efficiency of the thermosyphon. The result of natural cooling without any thermosyphon immersed in the container (Run 1) is shown as a base for comparison. It can be seen that the cooling rate is the slowest. All the results show that systems with the thermosyphons increased the cooling rate. For natural cooling (Run 1), it took nearly 2 hours to cool the water from 100 °C to 88 °C. With the type HP1 water cooled thermosyphon (Run 2) at the low coolant flow rate of 0.9 ml/s, 100 °C water was cooled to 60 °C in 2 hours. The same thermosyphon performed better at high coolant flow rate (Run 3) than with the low flow rate (Run 2) as expected. The results also show that force convection air cooling (Run 5) is better than natural convection air cooling (Run 4) for the type HP2 thermosyphon, as expected. From the results it would seem that the L-shaped type HP5 thermosyphon (Run 8) performed better than the straight pipe of type HP3 (Run 6) followed by the J-shape type HP4 (Run 7) unit. The difference in performance could be due to the shape of pipes. For the air cooled type HP2 & HP3 pipes, Run 6 with the longer condenser length performs better than the shorter one in Run 5. It should be pointed out here that the thermosyphons are of different sizes and the lengths of the evaporator sections that were immersed in the hot water varied from pipe to pipe as indicated in Table 1. Hence, in order to determine which geometry pipe performs better, it would be necessary to fabricate and compare pipes with the same equivalent sizes.

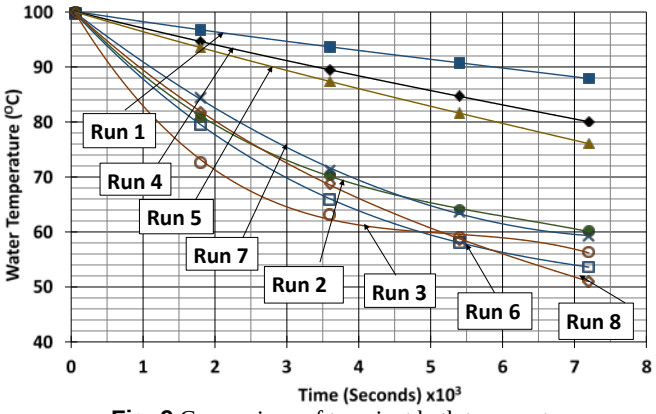

Fig. 9 Comparison of transient bath temperatures

5.4 Effect of coolant water flow rate and natural and force convection air cooling

The effect of coolant water flow rate and natural and force convection air cooling for Runs 2 to 5 are demonstrated in Fig. 10. Better performance results in lower container temperature as seen in Fig. 9 or greater heat removal rate from the container. The heat transfer rate results in Fig. 10 show that thermosyphons with higher coolant flow rate (Run 3) performed better than at low flow rate (Run 2). In the case of air cooling, thermosyphons with force convection air flow (Run 5) performed better than at natural convection (Run 4).

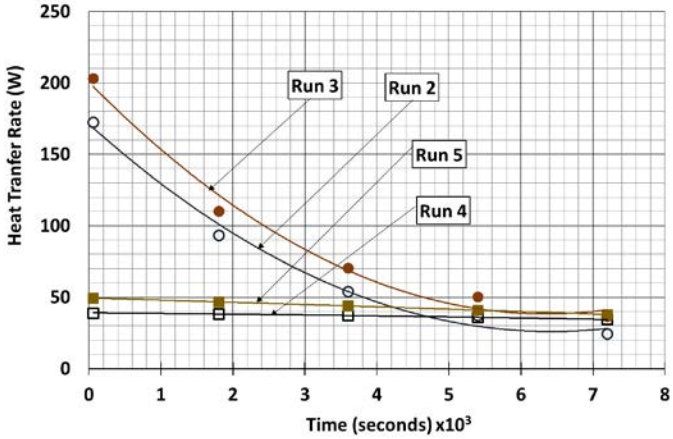

Fig. 10 Effect of coolant water flow rate and natural and force convection air cooling for Runs 2-5

Global Digital Central
ISSN: 2155-658X

6. Conclusions

A method to compare the performance of various thermosyphons rapidly and economically was proposed. The ease and simplicity of the procedure was demonstrated by cooling a container of hot water using various thermosyphons. From the results obtained it was found that force air convection cooling was better than natural convection and that high water flow rate was better than low flow rate.

NOMENCLATURE

A_{ins}	surface area of container (= 0.714 m^2)
A_e	surface area of evaporator section (m^2)
C_{pw}	specific heat of water (kJ/kg K)
D_e	external diameter of evaporator section (m)
h_a	natural convection heat loss (= 2 W/m^2 K)
L_{ad}	adiabatic length (m)
L_c	condenser length (m)
L_e	evaporator length (m)
T_a	ambient temperature (°C)
T_{ad1}, T_{ad2}	adiabatic temperatures (°C)
T_b	container water temperature (°C)
T_{fin1}, T_{fin2}	fin temperatures (°C)
T_{bu}, T_{bl}, T_w	water temperatures (°C)
Ti_{ns}	surface temperature of the insulation (°C)
T_{sat}	saturation temperature (°C)
T_{wi}, T_{wo}	coolant water inlet and outlet temperatures (°C)
T_w	mean coolant water temperature (°C)
W_b	mass of water in the container (kg)
$\dot{q}_b$	heat removed from container (kJ/s)
$\dot{q}_{ins}$	heat loss from container (kJ/s)
$\dot{q}_w$	heat transfer to coolant water (kJ/s)
ΔT_w, ΔT_m	mean difference between bath (evaporator) and coolant water temperature (condenser) (°C)
θ	inclination angle measured from the horizontal (degrees)
γ	ratio of heat transfer to the coolant/total heat removed from the containerl

REFERENCES

Anjakar, P.G. and Yarasu, D.R.B., 2012, "Experimental Analysis of Condenser Length Effect on the Performance of Thermosyphon," *International Journal of Emerging Technology and Advanced Engineering*, **2**, 494-499.

Buschmann, M. H. and Franzke, U., 2013, "Improvement of Thermosyphon Performance by Employing Nanofluid," *International Journal of Refrigeration*, **40**, 416-428.
http://dx.doi.org/10.1016/j.ijrefrig.2013.11.022

Celata, G.P., Cumo, M. and Furrer, M., 2010, "Experimental Tests of a Stainless Steel Loop Heat Pipe with Flat Evaporator," *Experimental Thermal and Fluid Science*, **34**, 866-878.
http://dx.doi.org/10.1016/j.expthermflusci.2010.02.001

Chang, S. W., Lo, D. C., Chiang, K. F. and Lin, C. Y., 2012, "Sub-atmospheric Boiling Heat Transfer and Thermal Performance of Two-Phase Loop Thermosyphon," *Experimental Thermal and Fluid Science*, **39**, 134-147.
http://dx.doi.org/10.1016/j.expthermflusci.2012.01.017

Huminic G., Huminic, A., Morjan, I. and Dunitrache, F., 2011, "Experimental Study of the Thermal Performance of Thermosyphon Heat Pipe Using Iron Oxide Nanoparticles," *International Journal of Heat and Mass Transfer*, **54**, 656-661.
http://dx.doi.org/10.1016/j.ijheatmasstransfer.2010.09.005

Huminic, G. and Huminic, A., 2011, "Heat Transfer Characteristics of a Two-phase Closed Thermosyphons Using Nanofluids," *Experimental Thermal and Fluid Science*, **35**, 550-557.
http://dx.doi.org/10.1016/j.expthermflusci.2010.12.009

Qu, J. and Wang, Q., 2013, "Experimental Study on the Thermal Performance of Vertical Closed-loop Oscillating Heat Pipes and Correlatiion Modeling," *Applied Energy*, **112**, 1154-1160.
http://dx.doi.org/10.1016/j.apenergy.2013.02.030

Shabgard, H., Xiao, B., Faghri, A., Gupta, R. and Weissman, W., 2014, "Thermal Characteristics of a Closed Thermosyphon under Various Filling Conditions," *International Journal of Heat and Mass Transfer*, **70**, 91-102.
http://dx.doi.org/10.1016/j.ijheatmasstransfer.2013.10.053

Solomon, A. B., Ramachandran, K. and Pillai B.C., 2012, "Thermal Performance of a Heat Pipe with Nanoparticles Coated Wick," *Applied Thermal Energy*, **36**, 106-112.
http://dx.doi.org/10.1016/j.applthermaleng.2011.12.004

Solomon, A. B., Mathew, A., Ramachandran, K., Pillai, B. C. and Karthikeyan, V. K., 2013, "Thermal Performance of Anodized Two Phase Closed Thermosyphon (TPCT)," *Experimental Thermal and Fluid Science*, **48**, 49-57.
http://dx.doi.org/10.1016/j.expthermflusci.2013.02.007

Wang J., 2009, "Experimental Investigation Of The Transient Thermal Performance of a Bent Heat Pipe with Grooved Surface," *Applied Energy*, **86**, 2030-2037.
http://dx.doi.org/10.1016/j.apenergy.2009.01.003